

X-ray properties of spiral galaxies

Roberto Soria

*Mullard Space Science Laboratory, University College London,
Holmbury St Mary, Surrey RH5 6NT, UK; rs1@mssl.ucl.ac.uk*

Abstract.

X-ray studies of nearby spiral galaxies with star formation allow us to investigate temperature and spatial distribution of the hot diffuse plasma, and to carry out individual and statistical studies of different classes of discrete sources (low- and high-mass X-ray binaries, Supernova remnants, supersoft and ultra-luminous sources). In particular, we briefly review the different models proposed to explain the ultra-luminous sources. We can then use the X-ray properties of a galaxy to probe its star formation history. We choose the starburst spiral M 83 to illustrate some of these issues.

1. Introduction

It is now thirty years since the first unambiguous identification of X-ray emission from our nearest giant spiral, M 31 (Margon, Lampton & Cruddace 1974). Today we know that X-ray emission in galaxies comes from discrete sources and hot diffuse gas. Discrete sources (accreting compact objects and SuperNova Remnants) are a fossil record of the stellar population, and may be used as a probe of star formation history. Diffuse X-ray emission is the tracer of the hot gas ($T > 10^6$ K) in galaxies and clusters; in galaxies, it is an indicator of recent star formation. Disentangling truly diffuse gas from faint, unresolved sources—such as faint X-ray binaries (XRBs), cataclysmic variables, coronal emission from main-sequence and T Tauri stars—is still a major problem, despite the fact that sensitivity and spatial resolution of the X-ray detectors have improved by three orders of magnitude since those early observations.

Today, X-ray studies of nearby galaxies can be conducted on two complementary levels. We can do a statistical study of the spatial and spectral distribution of the sources: this can help us distinguish between different physical classes of X-ray emitters. And we can use the X-ray sources as a tool to probe the structure and evolution of the host galaxy.

Statistical studies of X-ray sources in the Milky Way are hampered by the large relative uncertainty in the distance of most sources (often by a factor of two) and by our very incomplete view due to the large extinction in the Galactic plane. Population studies can be conducted more easily in nearby galaxies, with more favorable viewing angles and the same relative distance for all the sources. By studying a large sample of galaxies it is also possible to quantify how the X-ray properties of a galaxy depend on its structural type and level of star-

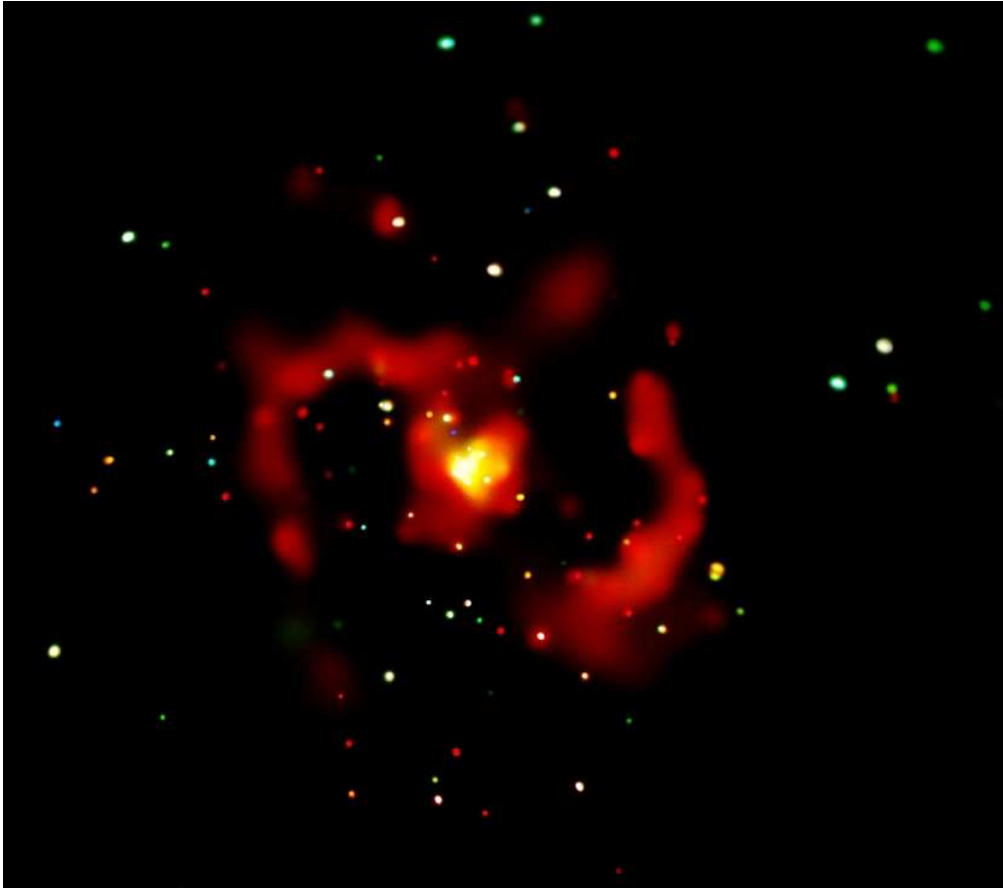


Figure 1. A true-color *Chandra*/ACIS image of M83 shows about 130 discrete sources and diffuse emission in the starburst nucleus and along the arms. The colors are: red = 0.3–1.0 keV; green = 1.0–2.0 keV; blue = 2.0–8.0 keV. Size of the image: $12' \times 10'$. North is up, East is left.

forming activity. Moreover, by quantifying the relation between observed X-ray properties and star formation history in nearby galaxies, one may predict the luminosity and color distribution of the faint galaxies detected in the Chandra Deep Field surveys (Giacconi et al. 2002), and therefore probe star formation at high redshift. (See R. Griffiths’s contribution elsewhere in these Proceedings.)

In this conference paper, I have chosen the starburst galaxy M83 to illustrate some of these issues. Located at a distance of ≈ 4 Mpc, M83 is a grand-design spiral seen at low inclination. More than 100 sources are resolved in a 51 ks *Chandra* observation. In addition to the point sources, a true-color image (Fig. 1) shows a bright starburst nucleus and strong, soft diffuse emission along the spiral arms.

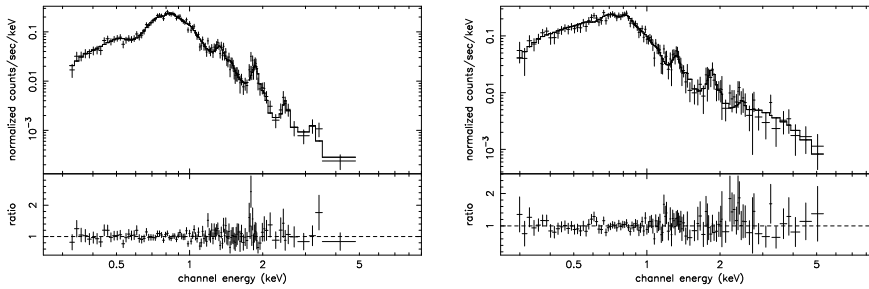


Figure 2. *Left:* the *Chandra*/ACIS spectrum of the unresolved emission in the starburst nucleus of M83 shows a thermal plasma component ($kT \approx 0.6$ keV, determined from the Fe L line complex) with strong metal lines; in particular, the 1.33 keV Mg XI line suggests that the gas has been enriched by core-collapse SNe. *Right:* the unresolved emission in the spiral arms has a larger contribution from cooler gas ($kT \approx 0.2$ keV) and a high-energy power-law component whose origin is yet to be determined.

2. Diffuse X-ray emission

The total X-ray luminosity emitted from M83 in the 0.3–8.0 keV band is $\approx 2.5 \times 10^{40}$ erg s $^{-1}$ ¹. Of this, $\approx 6 \times 10^{39}$ erg s $^{-1}$ comes from the resolved sources and the rest is unresolved. The nuclear starburst contributes for $\approx 5 \times 10^{39}$ erg s $^{-1}$ (of which $\approx 1 \times 10^{39}$ erg s $^{-1}$ from resolved sources). The unresolved X-ray emission is dominated by a multitemperature, optically thin plasma component, at $kT \sim 0.2$ –0.7 keV, slightly hotter in the nuclear region than in the arms (Figures 1, 2). It is likely to originate from gas shock-heated by core-collapse SN explosions². The unresolved emission from the disk region has a power-law-like tail that dominates above 3 keV. Its origin is still unclear: a population of faint, unresolved XRBs can produce a power-law component. The emission can also be due to a second thermal plasma component at $kT > 2$ keV, or to Compton upscattering of far-IR photons by relativistic electrons (Valinia & Marshall 1998).

From the observed temperature and luminosity, we estimate an average density $n_e \approx 5 \times 10^{-2}$ cm $^{-3}$ and a total mass $\sim 10^7 M_\odot$ for the X-ray emitting gas in M83; the cooling timescale is $\approx 10^8$ yr. For the hot gas in the starburst nuclear region, $n_e \approx 0.2$ cm $^{-3}$, $M \approx 5 \times 10^5 M_\odot$, $t_c \approx 4 \times 10^7$ yr. Hence, the hot gas is an indicator of recent star formation.

3. Discrete X-ray sources

¹In other bands: $L_B \approx 2.5 \times 10^{43}$ erg s $^{-1}$, $L_{\text{FIR}} \approx 2.5 \times 10^{43}$ erg s $^{-1}$, $L_{\text{H}\alpha} \approx 1.5 \times 10^{40}$ erg s $^{-1}$. In general, $L_X \sim L_{\text{H}\alpha} \sim 10^{-3} L_{\text{FIR}}$ for starburst spirals (Fabbiano & Shapley 2002; Calzetti et al. 1995; Condon et al. 1998; de Vaucouleurs et al. 1991); all three bands can be used as indicators of star formation.

²SN ejecta can easily provide $v_{\text{sh}} \sim T^{1/2} > 650$ km s $^{-1}$, required to heat the gas to $kT \gtrsim 0.5$ keV. Assuming a SN rate ~ 0.05 yr $^{-1}$ for M83, and a total mechanical energy $\approx 10^{51}$ erg injected into the ISM by each SN, the total mechanical luminosity is $\approx 1.5 \times 10^{42}$ erg s $^{-1}$.

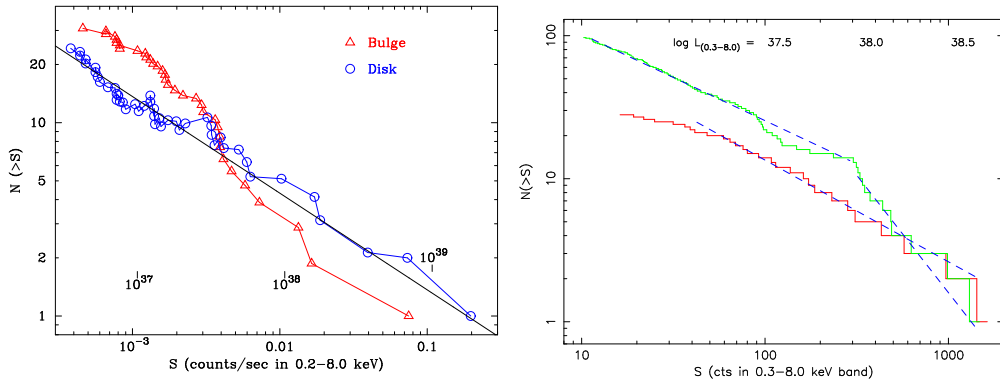


Figure 3. *Left:* the cumulative luminosity distribution of the discrete sources in M 81 shows a break at $L \approx 3 \times 10^{37}$ erg s $^{-1}$, suggesting that bulge sources belong to a much older population; continuous star formation in the disk results in an unbroken power-law instead (Tennant et al. 2001). *Right:* in M 83, the luminosity function of the sources inside the inner 60'' (nuclear starburst region + bar) does not show a break (lower curve). This can be interpreted as due to continuous star formation in the nuclear region. However, the luminosity function of the X-ray sources outside 60'' (upper curve) has a break at $L_x \approx 10^{38}$ erg s $^{-1}$, interpreted either as the upper limit of the NS population or as due to population aging (Soria & Wu 2002).

3.1. Population studies

Populations of discrete X-ray sources in different galaxies and different galactic environments (bulge, disk, spiral arms, etc.) have different morphologies for their luminosity distributions (Fig. 3). It has been suggested that the slope and the break are indicative of the star-formation history (Wu 2001): an unbroken power-law indicates continuous star formation; a break (ie, a lack of bright sources) may be caused by aging of the X-ray source population, indicating the look-back time to the last major episode of star formation. This in turn provides information on the dynamical history of a galaxy, because star formation is often triggered by close encounters and mergers with other galaxies.

Color-color plots can separate different classes of X-ray sources, and distinguish XRBs in the soft and hard state (Fig. 4). XRBs are, in turn, a mixture of young (timescale of $\sim 10^7$ yr after star formation), wind-accreting, high-mass XRBs (generally seen through higher intrinsic absorption), and old (timescale of $\sim 10^9$ yr after star formation), Roche-lobe accreting low-mass XRBs. For Galactic sources, the color and spectral separation between the hard and soft state is generally larger in XRBs with a BH accretor than in those with a NS.

Studies of luminosity and color variability offer another criterion to separate XRBs (which often show state transitions) from SNRs (which do not). The age of different classes of X-ray sources can be inferred from a study of their spatial correlation with various indicators of recent star formation, eg, the spiral arms defined by the H II regions (Fig. 5).

3.2. The nature of individual sources

In M 83, detailed spectral analysis is possible for sources with an emitted luminosity $\gtrsim 10^{38}$ erg s $^{-1}$. We can easily distinguish (Fig. 6):

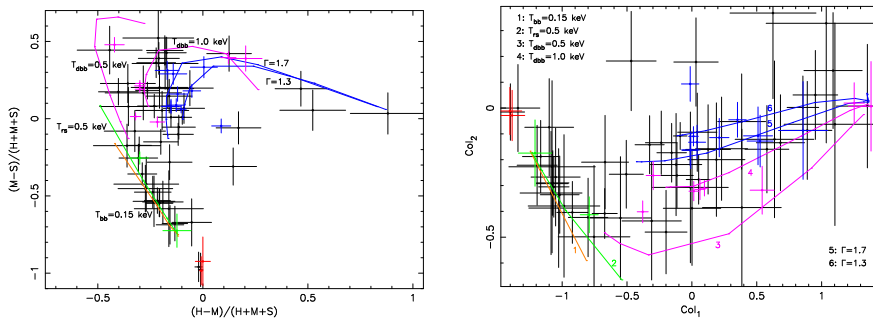


Figure 4. *Left:* The model lines in the X-ray color-color diagram constrain the expected locations (for $4 \times 10^{20} \leq n_H \leq 5 \times 10^{22} \text{ cm}^{-2}$) of different classes of X-ray sources in M83: XRBs in a hard state (power-law spectrum with $1.3 \lesssim \Gamma \lesssim 1.7$), XRBs in a soft state (diskbb with $0.5 \lesssim kT \lesssim 1.0 \text{ keV}$), SNRs (Raymond-Smith thermal spectrum with $kT \approx 0.5 \text{ keV}$), supersoft sources (blackbody spectrum with $kT \approx 0.06 \text{ keV}$). Here $S = 0.3\text{--}1.0 \text{ keV}$, $M = 1.0\text{--}2.0 \text{ keV}$, $H = 2.0\text{--}8.0 \text{ keV}$. For the brightest sources, we can obtain individual spectral fits. Datapoints of sources whose X-ray spectra are consistent with hard-state XRBs have been plotted in blue; plotted in magenta: soft-state XRBs; in green: SNRs; in red: supersoft sources. *Right:* Same model lines, for a different choice of X-ray colors. Here $\text{Col}_1 \equiv (CH + CM)/\sqrt{2}$, $\text{Col}_2 \equiv (CH - CM)/\sqrt{2}$, where $CH = (H - S)/(H + S)$, $CM = (M - S)/(M + S)$.

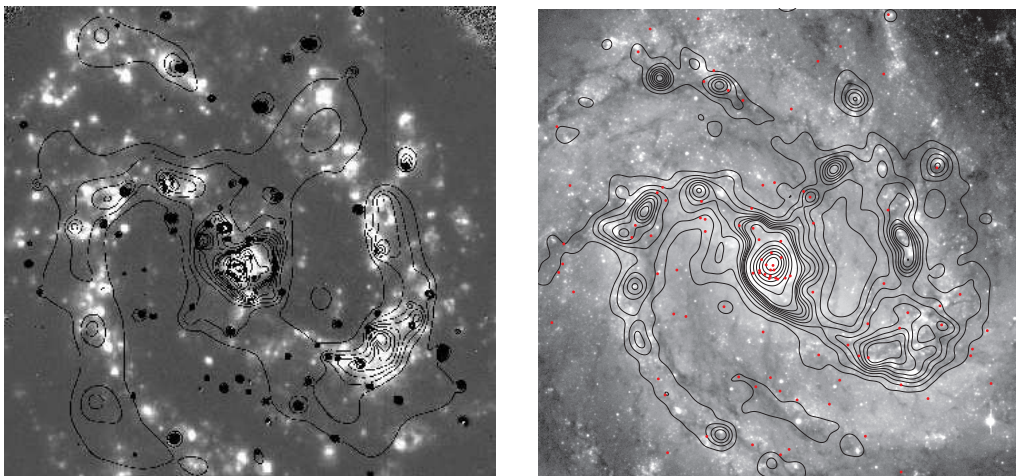


Figure 5. *Left:* the diffuse X-ray emission (0.3–8.0 keV *Chandra* contours) is associated to the spiral arms and is an indicator of recent star formation, similar to the $H\alpha$ emission (greyscale image from the Anglo-Australian Telescope). *Right:* Most of the discrete X-ray sources (red circles) are associated with star-forming regions or young stellar populations (greyscale VLT B-band image, tracing OBA stars). The radio flux (12 cm contours from a VLA image) is a combination of free-free and synchrotron emission and is also an indicator of star formation. Size of both images: $6' \times 6'$. North is up, East is left.

- the X-ray nucleus, coincident with the optical/IR nucleus. Its spectrum is consistent with that of a supermassive black hole accreting well below its Eddington rate ($L_x \approx 2 \times 10^{38} \text{ erg s}^{-1}$; $M \sim 10^7 M_\odot$);
- XRBs in a hard state: their X-ray spectrum is well fitted with a simple power law of photon index ≈ 1.3 – 1.7 ;
- XRBs in a soft state: their X-ray spectra is softer, dominated by a blackbody or disk-blackbody at $0.5 \lesssim kT \lesssim 1$, plus a power law of photon index ≈ 2.2 – 3.0 (due to Compton upscattering of the disk photons);
- “emission-line” sources: they show a few prominent metal lines (in particular from Si and Mg). The softer sources are more likely to be young SNRs; the harder ones could be X-ray binaries surrounded by a photoionized nebulae or stellar wind. They latter class would then be analogous to Vela X-1 or Cen X-3 in our Galaxy (eg, Liedahl et al. 2000);
- bright supersoft sources, characterized by a thermal spectrum with blackbody temperature $kT \approx 60 \text{ eV}$. They are generally interpreted as accreting white dwarfs with stable nuclear burning on their surface (see also Di Stefano & Kong 2003).

For a more extensive discussion of the spectral and temporal properties of the discrete sources in M 83, see Soria & Wu (2003).

The brightest point source, located $\approx 5'$ south-east of the nucleus, is variable and has an emitted luminosity of $\approx 10^{39} \text{ erg s}^{-1}$ (Fig. 6, bottom panels). Hence, it can be classified as an ultra-luminous source (ULX).

4. Ultra-luminous sources

4.1. X-ray observations

The maximum luminosity of an accreting source is known as Eddington limit:

$$L_{\text{Edd}} = \frac{4\pi cGM}{\langle \kappa \rangle} = 1.3 \times 10^{38} \left(\frac{\kappa_{\text{Th}}}{\langle \kappa \rangle} \right) \left(\frac{M}{M_\odot} \right) \text{ erg s}^{-1}.$$

where $\langle \kappa \rangle$ is the average flux-weighted opacity.

The term “ULX” is generally applied to X-ray sources outside a galactic nucleus which persistently exceed (when in an active state) the Eddington luminosity of a $7M_\odot$ BH (thought to be the “canonical” BH mass value); some sources emit a luminosity of up to a few times $10^{40} \text{ erg s}^{-1}$ (Roberts & Warwick 2000). In fact, it is necessary to distinguish between bright SNR (for which the Eddington limit does not apply) and accreting sources. Even in the absence of detailed spectral information, variability by a factor $\gtrsim 2$ is usually taken as a good indicator that a source is not an SNR. Correlation with a non-thermal radio source is another criterion to identify an SNR.

It is still unclear whether ultra-luminous accreting sources are simply the high-luminosity end of the X-ray binary population, or a different physical class of objects. No significant break or feature at $L \approx 10^{39} \text{ erg s}^{-1}$ is found in the

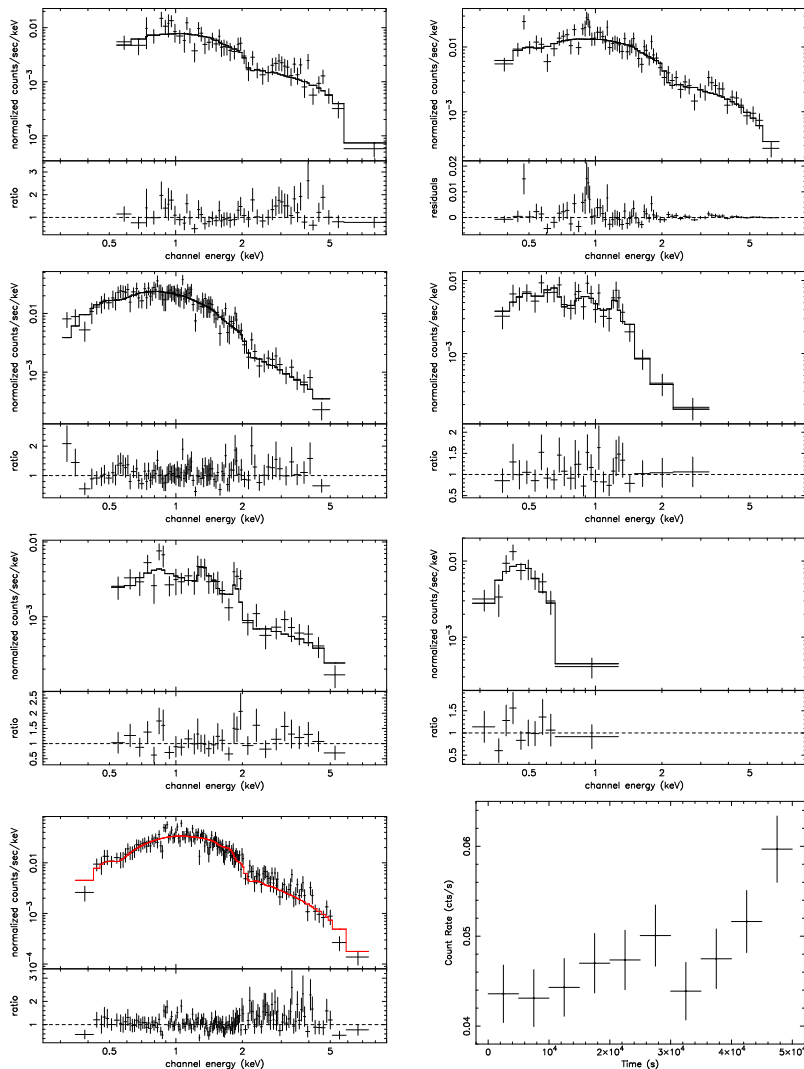


Figure 6. Spectral fits to a sample of bright X-ray sources in M83 show different classes of objects. First three rows, from top left: the galactic nucleus; an X-ray binary in a hard state; an X-ray binary in a soft state; a source with soft thermal plasma emission (a young SNR?); a source with a power-law continuum plus line emission (from a photo-ionized stellar wind?); a supersoft source. See Soria & Wu (2003) for further details on the sources and their fitted spectral models. Bottom row: the brightest X-ray source in M83 has an emitted luminosity in excess of 10^{39} erg s^{-1} . A power-law spectral fit gives a photon index 2.5 ± 0.1 . Its lightcurve shows an increase by $\approx 40\%$ over the duration of the *Chandra* observation.

cumulative luminosity distribution of X-ray sources in galaxies which contain ULXs. However, the statistical error is large, due to the small number of sources in each galaxy above that luminosity.

ULXs are found in elliptical galaxies (eg, NGC 1553: Sarazin et al. 2000; NGC 4697: Blanton, Sarazin & Irwin 2001), associated with an old stellar population, often inside globular clusters. Their location, and the steep slope of the high-luminosity end of the X-ray luminosity function suggest that, in this case, they are old systems accreting from a low-mass companion. On the other hand, ULXs are also often found in starburst or active star-forming galaxies (eg, M82: Matsumoto et al. 2001; the Antennae: Zezas & Fabbiano 2002). The X-ray luminosity function in these galaxies is typically an unbroken power-law with a flat slope, dominated at high luminosities by young high-mass XRBs. In this case, the ULXs appear to be associated with a very young stellar population.

X-ray spectral analyses do not provide a unique physical identification, either. Some ULXs can be fitted with a simple power law continuum (La Parola et al. 2001; Strickland et al. 2001). Others are better fitted with a disk-blackbody model (Makishima et al. 2000; Roberts et al. 2002) with color temperatures $\approx 1\text{--}1.5$ keV (such high color temperatures can still be consistent with a high-mass accretor, if the spectral hardening factor is ≈ 3). Transitions from a hard to a soft state are seen in a few cases (Kubota et al. 2001), analogous to those detected in Galactic BH candidates. At least one ULX has a supersoft spectrum with a blackbody temperature of ≈ 80 eV (Swartz et al. 2002). Finally, X-ray variability studies have shown a range of different behaviours: most of the sources are persistent; a few are transients on timescales of a few months/years; others are highly variable on timescales of a few thousand seconds (a ULX in M74: M. Garcia 2002, priv. comm.)

4.2. Three physical models for the ULXs

There are at least three models to explain the physical nature of the ULXs (having excluded the bright X-ray SNRs from this category):

- **Intermediate-mass black holes (IMBHs).**

The Eddington limit is proportional to the mass of the accreting object, hence a $100\text{-}M_{\odot}$ BH could have a persistent luminosity $\gtrsim 10^{40}$ erg s^{-1} . The first problem this model has to address is how to form them. It is still not known what the maximum mass is for BHs formed via SN explosions of single stars, and how this mass depends on the metallicity of the progenitor star. If BH masses $\gtrsim 50M_{\odot}$ are required to explain the observations, mergers of smaller-scale bodies in a dense environment are likely to be necessary. It has been shown (Sigurdsson & Hernquist 1993; Kulkarni, Hut, & McMillan 1993) that it is not possible to merge small ($M \lesssim 50M_{\odot}$) BHs in a globular cluster via three body interactions: recoils tend to kick the BHs out of the cluster before they can merge. However, mergers become possible if one considers four-body interactions (Miller & Hamilton 2002). The best chance to form an IMBH occurs if a number of progenitor stars coalesce first into a $\sim 10^3 M_{\odot}$ star which would then undergo a SN explosion (Ebisuzaki et al. 2001). In this case, the formation process would be most likely to occur near the center of compact, young super-star clusters usually found in starburst galaxies. If super-star

clusters are the progenitors of globular clusters, this could also explain the presence of IMBHs in the old globulars of elliptical galaxies. Yet another suggestion (Madau & Rees 2001) is that IMBHs could be pre-galactic remnants formed from the fragmentation of primordial molecular clouds. The second problem to address is how to feed them: a discussion on the mass transfer mechanism (Roche-lobe overflow or stellar wind) and allowed ranges of mass for the companion star is beyond the scope of this review. (See Zezas & Fabbiano 2002 for such a discussion regarding the ULXs in M 82). Thirdly, how to observe them. The most reliable determination of the mass function for Galactic BHs comes from optical observations of photometric variations and line velocity shifts of the accretion disk and companion star over a binary period. It is of course more difficult to achieve that in other galaxies (for M 83, distance modulus ≈ 28).

- **Beating the Eddington limit**

The classical Eddington limit assumes that the average opacity $\langle \kappa \rangle \geq \kappa_{\text{Th}}$. However, this may not be the case if the radiating medium (accretion disk or stellar surface) is clumpy. It can be shown that the flux-weighted, volume-averaged opacity can be lower than the electron scattering opacity for an inhomogeneous medium (Shaviv 1998). If this is the case, more photons can escape without blowing away the accretion flow, so that steady-state luminosities $\sim 10^{40}$ erg s $^{-1}$ could in principle be attained by a stellar-mass BH with $M \lesssim 10M_{\odot}$. Observational evidence for “super-Eddington” luminosities has been suggested in the case of novae (Shaviv 2001). Models of clumpy accretion disks based on the same principle have also been proposed (Begelman 2002). At $L \approx L_{\text{Edd}}$, all systems should develop strong radiation-driven winds, whose density and velocity could in principle be inferred from high-resolution UV and X-ray spectra.

- **Beamed emitters**

If the X-ray emission is beamed towards us rather than isotropic, the estimated ULX luminosities can be scaled down, depending on the beaming factor. Beamed X-ray emission is known to occur in some microquasars (eg, GRS 1915+105). Such systems would appear highly super-Eddington if we happen to observe them pole-on (Fabrika & Mescheryakov 2001; King et al. 2001). It is sometimes possible to determine whether the X-ray emission is beamed by studying the optical spectral lines of the photoionized nebula around a ULX. A detailed discussion of this technique is presented by M. Pakull elsewhere in these Proceedings.

Acknowledgements

Thanks to Kinwah Wu, Rosanne Di Stefano, Albert Kong, Manfred Pakull, Andrea Prestwich, Doug Swartz for comments and discussions, to Stuart Ryder for the use of his AAT images, and to Reiner Beck for his VLA radio map.

References

- Begelman, M. C. 2002, 568, L97
 Blanton, E. L., Sarazin, C. L., & Irwin, J. A. 2001, ApJ, 552, 106

- Calzetti, D., Bohlin, R. C., Kinney, A. L., Storchi-Bergmann, T., & Heckman, T. M. 1995, *ApJ*, 443, 136
- Condon, J. J., Yin, Q. F., Thuan, T. X., & Boller, Th. 1998, *AJ*, 116, 2682
- de Vaucouleurs, G., de Vaucouleurs, A., Buta, H. G., Paturel, G., & Fouque, P. 1991, in the Third General Catalogue of Bright Galaxies
- Di Stefano, R., & Kong, A. K. H. 2003, *ApJ*, submitted
- Ebisuzaki, T. et al. 2001, *ApJ*, 562, L19
- Fabbiano, G., & Shapley, A. 2002, *ApJ*, 565, 908
- Fabrika, S., & Mescheryakov, A. 2001, in “Galaxies and their Constituents at the Highest Angular Resolutions”, Proceedings of the IAU Symposium 205 (Manchester, 15-18 August 2000), p. 268 (astro-ph/0103070)
- Giacconi, R., et al. 2002, *ApJS*, 139, 369
- King, A. R., Davies, M. B., Ward, M. J., Fabbiano, G., & Elvis, M. 2001, *ApJ*, 552, L109
- Kubota, A., Mizuno, T., Makishima, K., Fukazawa, Y., Kotoku, J., Ohnishi, T., & Tashiro, M. 2001, *ApJ*, 547, L119
- Kulkarni, S. R., Hut, P., & McMillan, S. L. W. 1993, *Nature*, 364, 421
- La Parola, V., Peres, G., Fabbiano, G., Kim, D. W., & Bocchino, F. 2001, *ApJ*, 556, 47
- Liedahl, D. A., Sako, M., Wojdowski, P. S., Paerels, F., & Kahn, S. M. 2000, *Revista Mexicana de Astronomia y Astrofisica*, 9, 40
- Madau, P., & Rees, M. J. 2001, *ApJ*, 551, 27
- Makishima et al. 2000, *ApJ*, 535, 632
- Margon, B., Lampton, M., & Cruddace, R. 1974, *ApJ*, 190, 285
- Matsumoto, H., Tsuru, T. G., Koyama, K., Awaki, H., Canizares, C. R., Kawai, N., Matsushita, S., & Kawabe, R. 2001, *ApJ*, 457, L25
- Miller, M. C., & Hamilton, D. P. 2002, *ApJ*, 576, 894
- Pakull, M. W., & Mirioni, L. 2002, in the proceedings of the symposium “New Visions of the X-ray Universe in the *XMM-Newton* and *Chandra* Era”, 26-30 November 2001, ESTEC, The Netherlands (astro-ph/0202488)
- Roberts, T. P., & Warwick, R. S. 2000, *MNRAS*, 315, 98
- Roberts, T. P., Warwick, R. S., Ward, M. J., & Murray, S. S. 2002, *MNRAS*, in press (astro-ph/0208196)
- Roberts, T. P., Goad, M. R., Ward, M. J., Warwick, R. S., O’Brien, P. T., Lira, P., & Hands, A. D. P. 2001, *MNRAS*, 325, L7
- Sarazin, C. L., Irwin, J. A., & Bregman, J. N. 2000, *ApJ*, 544, L101
- Shaviv, N. J. 1998, *ApJ*, 494, L193
- Shaviv, N. J. 2001, *MNRAS*, 326, 126
- Soria, R., & Wu, K., 2002, *A&A*, 384, 99
- Soria, R., & Wu, K., 2003, *A&A*, submitted
- Sigurdsson, S., & Hernquist L. 1993, *Nature*, 364, 423
- Strickland, D. K., Colbert, E. J. M., Heckman, T. M., Weaver, K. A., Dahlem, & M. Stevens, I. R. 2001, *ApJ*, 560, 707
- Swartz, D., Ghosh, K., Suleimanov, V., Tennant, A., & Wu, K. 2002, *ApJ*, in press (astro-ph/0203487)
- Tennant, A. F., Wu, K., Ghosh, K. K., Kolodziejczak, J. J., & Swartz, D. A. 2001, *ApJ*, 549, L43
- Valinia, A., & Marshall, F. E. 1998, *ApJ*, 505, 134
- Wu, K. 2001, *PASA*, 18, 443
- Zezas, A., & Fabbiano, G. 2002, *ApJ*, 577, 726